



ELSEVIER

Journal of Crystal Growth 235 (2002) 161–166

JOURNAL OF  
**CRYSTAL  
GROWTH**

www.elsevier.com/locate/jcrysgr

## Defect density characterization of detached-grown germanium crystals

M. Schweizer<sup>a,\*</sup>, S.D. Cobb<sup>b</sup>, M.P. Volz<sup>b</sup>, J. Szoke<sup>a,c</sup>, F.R. Szofran<sup>b</sup>

<sup>a</sup> *USRA, NASA-MSFC, SD47, Huntsville, AL 35812, USA*

<sup>b</sup> *NASA-MSFC, SD47, Huntsville, AL 35812, USA*

<sup>c</sup> *University of Miskolc, H-3515 Miskolc-Egyetemvaros, Hungary*

Received 14 August 2001; accepted 6 November 2001

Communicated by K.W. Benz

### Abstract

Several (1 1 1)-oriented, Ga-doped germanium crystals were grown in pyrolytic boron nitride (pBN) containers by the Bridgman and the detached Bridgman growth techniques. Growth experiments in closed-bottom pBN containers resulted in nearly completely detached-grown crystals, because the gas pressure below the melt can build up to a higher pressure than above the melt. With open-bottom tubes the gas pressure above and below the melt is balanced during the experiment, and thus no additional force supports the detachment. In this case the crystals grew attached to the wall. Etch pit density (EPD) measurements along the axial growth direction indicated a strong improvement of the crystal quality of the detached-grown samples compared to the attached samples. Starting in the seed with an EPD of  $6\text{--}8 \times 10^3 \text{ cm}^{-2}$  it decreased in the detached-grown crystals continuously to about  $200\text{--}500 \text{ cm}^{-2}$ . No significant radial difference between the EPD on the edge and the middle of these crystals exists. In the attached grown samples the EPD increases up to a value of about  $2\text{--}4 \times 10^4 \text{ cm}^{-2}$  (near the edge) and up to  $1 \times 10^4 \text{ cm}^{-2}$  in the middle of the sample. Thus the difference between the detached- and the attached-grown crystals with respect to the EPD is approximately two orders of magnitude. © 2002 Published by Elsevier Science B.V.

**Keywords:** A1. Defects; A2. Bridgman technique; A2. Detached Bridgman technique; A2. Single crystal growth; B2. Semiconducting germanium

### 1. Introduction

During normal Bridgman growth experiments the melt and the growing crystal are in contact with the ampoule wall. Different expansion

coefficients of the ampoule material and the crystal lead to stress in the crystal, which can result in an increased defect density near the edge or even in cracks in the grown crystal.

In recent years many authors reported less than complete ampoule-crystal contact during directional solidification experiments, especially under microgravity conditions [1–3]. In this so-called detached or dewetting growth process, a small gap between the growing crystal and the ampoule

\*Corresponding author. Tel.: +1-256-544-4167; fax: +1-256-544-8762.

E-mail address: markus.schweizer@msfc.nasa.gov (M. Schweizer).

container exists. The gap thickness and the stability of the wall-free growth depend primarily on the wetting behavior between the melt and the container material (expressed through the contact angle  $\theta$ ), the growth angle  $\alpha$  of the crystal, and external forces, which can change the meniscus shape of the growing crystal. Without consideration of external forces, detachment will occur if the sum of the contact angle  $\theta$  and the growth angle  $\alpha$  is equal or larger than  $180^\circ$  [4,5], which follows from geometrical considerations. In Fig. 1a schematic drawing of the detached Bridgman growth technique is given.

A detailed explanation and reviews about the detached growth process are given e.g. by Regel and Wilcox [1] and Duffar et al. [4]. It is expected that detached growth will improve the crystal quality. Larson et al. demonstrated this expected defect density reduction quantitatively by growing Cd(Zn)Te crystals with only partial wall contact in graphite coated quartz glass ampoules under microgravity conditions [6,7]. Recently, Dold et al. observed in the wall free grown areas of a partly detached-grown germanium crystal a EPD reduction of more than one order of magnitude [8].

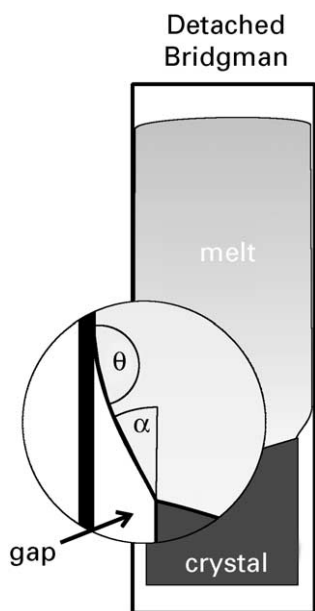


Fig. 1. Schematic drawing of the detached growth process.

The experiment was performed in a mirror furnace in a quartz ampoule under terrestrial conditions.

Also Duffar et al. [9,10] have grown nearly completely detached GaSb-crystals in quartz glass ampoules under Earth conditions. Detachment was achieved with an additional active pressure control system and in another case with the regulation of the furnace temperature profile in order to generate a gas pressure difference above and below the melt inside the ampoule. The last method with the temperature profile regulation was also successfully utilized in our own group by growing detached GeSi crystals [11,12].

Compared to the quartz glass ampoules utilized by Dold et al, Duffar et al. and Larson et al., the pyrolytic boron nitride (pBN) containers used by our group offer the advantage of a particularly favorable wetting behavior. For Ge on a pBN substrate, Kaiser et al. measured a contact angle  $\theta$  of  $173 \pm 3^\circ$  [13]. Considering the growth angle  $\alpha$  for germanium of  $7\text{--}13^\circ$  [14], we are near the condition to get detachment with  $\theta + \alpha \geq 180^\circ$ . However, due to a larger expansion coefficient of pBN crucibles ( $3 \times 10^{-6} \text{ K}^{-1}$  in the *a*-direction and  $30 \times 10^{-6} \text{ K}^{-1}$  in the *c*-direction) compared to quartz ( $0.5 \times 10^{-6} \text{ K}^{-1}$ ), it was still an open question if the crystal quality would be improved in samples grown detached in pBN containers.

The aim of this paper is to describe the first results of detached-grown germanium single crystals. A detailed description of the variation of the EPD along the crystal growth axis will be given and the results will be compared to those for a reference crystal grown under attached conditions.

## 2. Experimental procedure

The detached growth experiments were performed in the Universal Multizone Crystallizer (UMC), a translation-free multizone furnace. A detailed description of the furnace is given in Ref. [15]. Undoped, (111)-oriented germanium crystals, 12 mm in diameter were used as seed material. The regrown crystals were doped to about  $8 \times 10^{18} \text{ at/cm}^3$  by the addition of Ga metal. The etch pit density distribution in the seed is between  $6\text{--}8 \times 10^3 \text{ cm}^{-2}$  (see Fig. 2). All crystals were

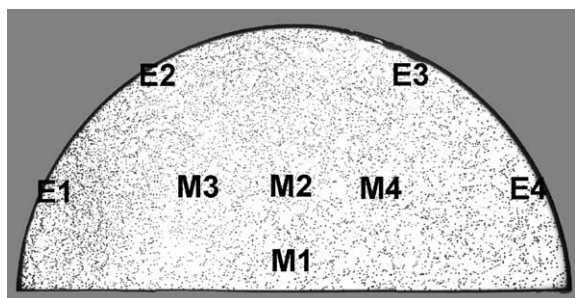


Fig. 2. Etched radial wafer from the seed crystal with a EPD around  $6\text{--}8 \times 10^3 \text{ cm}^{-2}$ . M1–M4 denotes the regions used to determine the EPD in the middle of the crystal and E1–E4 along the edge.

grown in pBN containers, sealed in quartz glass ampoules. For the detached growth experiments closed-bottom crucibles were utilized. Thus it was possible to obtain a maximum pressure difference approximately equal to the hydrostatic pressure of the molten sample [12]. For reference conditions an attached crystal in an open-bottom pBN crucible was grown under otherwise similar conditions. An extensive discussion about the different containers and their influence on the detachment is given in Ref. [12]. Before the experiments, the pBN containers and the quartz glass ampoules were cleaned with acetone and methanol and rinsed with distilled water several times. The ampoules were baked out together with the pBN containers under vacuum at  $1050^\circ\text{C}$ . The Ge-crystals were also cleaned in acetone and methanol, rinsed with water and etched in 18:8:5 polishing etch ( $\text{HNO}_3$ ;  $\text{CH}_3\text{COOH}$ ;  $\text{HF}$ ). Finally the complete growth ampoule assembly was sealed under forming gas (Argon containing 2%  $\text{H}_2$ ) or vacuum ( $2 \times 10^{-6} \text{ mbar}$ ).

At the beginning of every experiment, the temperature profile was adjusted to melt the feed crystal, beginning at the top, until a seed crystal with a typical length of  $\approx 20 \text{ mm}$  remained unmelted. All growth experiments were performed by moving the temperature profile through the sample at  $5 \text{ mm/h}$  by zone programming. The temperature gradient measured with thermocouples outside the ampoule during the growth was between 20 and  $25 \text{ K/cm}$ . The length of the grown

crystals was between 45 and 60 mm. The surface of the grown crystal was analyzed by optical and scanning electron microscopy and the surface roughness was measured using a profilometer. After the surface measurements were completed, an axial slab approximately 1.5 mm thick was cut from each crystal. From the two remaining D-shaped pieces, radial wafers (111)-oriented were prepared. They were polished with 15, 9, and  $1 \mu\text{m}$  diamond paste and SYTON<sup>TM</sup>. To reveal the etch pit density distribution, the slices were etched for 10 minutes with the Billig etchant [16] which is 12 g KOH and 8 g  $\text{K}_3[\text{Fe}(\text{CN})_6]$  dissolved in 100 ml  $\text{H}_2\text{O}$  at approximately  $85^\circ\text{C}$ .

### 3. Results

It was possible to reproducibly grow detached single germanium crystals without any external active pressure control system. After opening the ampoules the grown crystals slipped easily out of the pBN-container. On each detached-grown crystal three growth facets are visible on the shiny surface, which are an indication of the single crystallinity (for the (111)-oriented crystals) and the wall-free growth. The single crystallinity was further proven by electron backscattering measurements and by chemical etching of the axial slice. Typical gap thickness between the detached-grown crystals and the ampoule wall is in the range of  $10 \mu\text{m}$ . The crystal surface roughness was measured with a profilometer. Only a few isolated very small islands with a size below approximately  $200 \mu\text{m}$  grew attached to the wall. The occurrence of such attached islands as well as their importance for the detached growth phenomenon are under investigation.

For reference conditions one attached crystal was grown in an open-bottom pBN tube, in which no pressure difference between the top of the melt and below the melt meniscus is possible [12]. However, in this attached-grown crystal small-detached areas also exist. The surface roughness on this crystal varies within  $\pm 5 \mu\text{m}$ .

Four-point resistivity measurements were performed on the axial slices of both the detached- and attached-grown crystals. There is no differ-

ence in the axial macrosegregation between the detached- and attached-grown crystals. All measurements followed the theoretical behavior for complete mixing expressed through the Scheil equation [17]. Etching the axial slice to detect microscopic dopant inhomogeneities revealed only the meltback interface curvature and some very weak striations in the last few millimeters of the crystal due to the influence of Marangoni convection near the area at the top of the melt. In accordance with the experiment performed by Dold et al. [7] no other striations due to time dependent buoyancy or Marangoni convection were detected in the grown crystals.

Three detached-grown crystals (UMC3, UMC5, UMC7) and one attached-grown crystal (UMC6) were characterized to determine the etch pit density (EPD). After cutting the crystals along the growth axis, radial slices in one of the remaining D sections were cut, polished, and etched. In Fig. 2, an etched slice from the seed crystal with the typical seed EPD distribution is shown. To determine the EPD on each slice, four micrograph-spots from the middle (compare Fig. 1, M1–M4) and from the edge (E1–E4 in Fig. 2) of the crystal were taken, the etch pits counted, and the average computed. There is no measurable difference between the edge and the middle of the seed crystal with an EPD of  $6\text{--}8 \times 10^3 \text{ cm}^{-2}$ . After the growth started in the detached-grown crystals the defect density decreases at the edge as well as in the middle of the crystals (compare Figs. 3 and 4—closed symbols). On the edge a lower value around  $200 \text{ cm}^{-2}$  is reached after a grown length of 10–15 mm, and in the middle of the crystal a value of approximately  $500 \text{ cm}^{-2}$  is reached after 15–20 mm (Fig. 4). In the attached-grown crystal (open symbols in Figs. 3 and 4) the EPD near the edge increases continuously from the seed-value up to approximately  $3.5 \times 10^4 \text{ cm}^{-2}$ . Thus a difference of more than two orders of magnitude is observed between the detached- and attached-grown crystals. The influence of the attachment on the defect density is also noticeable in the middle of the attached grown crystal. After a reduction in the first grown millimeters the EPD increases up to a value around  $1 \times 10^4 \text{ cm}^{-2}$ .

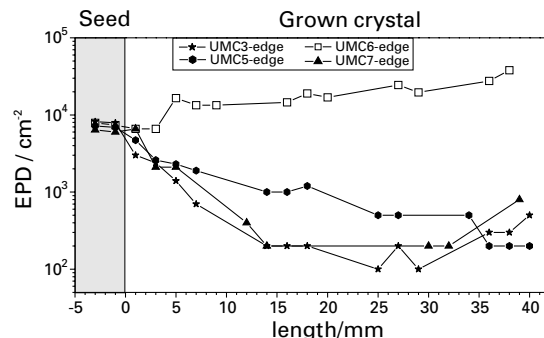


Fig. 3. Axial EPD variation along the edge in detached- (closed symbols) and attached-grown (open symbols) crystals. In the detached-grown crystals the EPD is reduced more than two orders of magnitude compared to the attached-grown crystal UMC6.

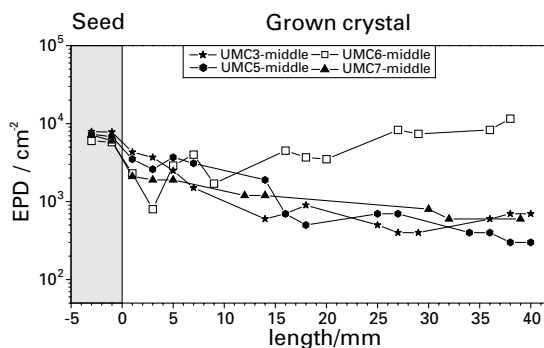


Fig. 4. Axial EPD variation in the middle in detached- (closed symbols) and attached-grown (open symbols) crystals.

In Fig. 5 micrographs from the detached grown crystal UMC7 (left hand side) and from the attached grown crystal UMC6 illustrate again the big difference in the EPD. Both crystal slices correspond to a growth length of 35 mm. The frequently observed initiation of polycrystalline growth in many other materials at the edge of attached crystals is due to a very high localized defect structure. The direct influence of attachment can be displayed through Fig. 6. After a growth length of 40 mm the crystal (UMC2) attaches locally to the wall, which was verified through a changed surface roughness by the optical microscope. In this local attached area, the EPD increases rapidly from a value around

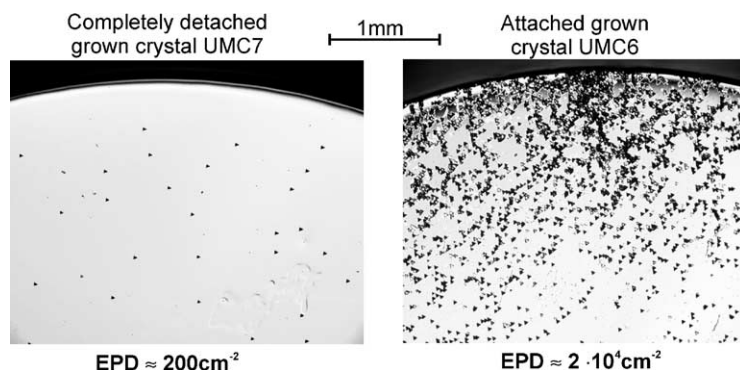


Fig. 5. Micrograph from the detached-grown sample UMC7 and from the attached-grown sample UMC6.

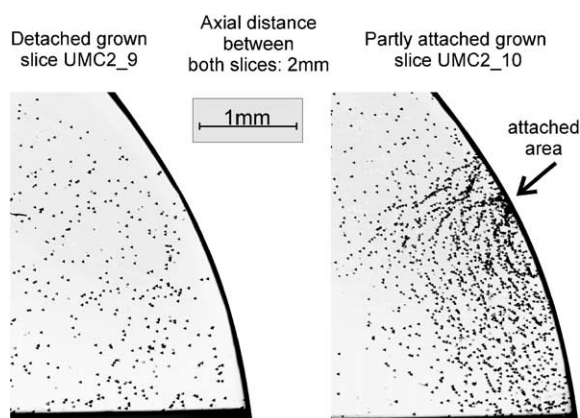


Fig. 6. Localized increased EPD after the crystal attaches partially to the wall.

$1 \times 10^3 \text{ cm}^{-2}$  up to around  $1\text{--}2 \times 10^4 \text{ cm}^{-2}$ . The axial distance between these two slices is 2 mm.

#### 4. Summary

It was possible to grow germanium single crystals reproducibly detached with the described growth technique. Due to the favorable wetting behaviour of the pBN-containers no active pressure control was necessary. The typical gap thickness of the detachment is around  $10 \mu\text{m}$ . No difference in the axial dopant macrosegregation was detectable between the detached- and attached-grown crystals.

For the first time, the improvement of detached crystals grown in pBN containers is demonstrated quantitatively. The etch pit density near the edge of the detached-grown crystals is  $200 \text{ cm}^{-2}$ , reduced by more than two orders of magnitude compared to the attached-grown crystal. Also in the middle of the detached-grown crystal the quality improvement is obvious: starting with a seed EPD of  $7 \times 10^3 \text{ cm}^{-2}$  it is reduced to a value below  $500 \text{ cm}^{-2}$ . In the middle of the attached-grown crystal the EPD is around  $1 \times 10^4 \text{ cm}^{-2}$ .

#### Acknowledgements

The authors are indebted to P. Carpenter for assistance in microscopic work and S. Gallop and P. Pettigrew for sample polishing and help in sample characterization, respectively. This work was supported by the NASA Physical Sciences Research Division.

#### References

- [1] L.L. Regel, W.R. Wilcox, *Microgravity Sci. Technol.* XI/4 (1998) 152.
- [2] I. Harter, T. Duffar, P. Dusserre, *Proceedings of the VIIth European Symposium on Materials and Fluid Sciences in Microgravity*, ESA SP-295, Oxford, UK, 1989, p. 69.
- [3] P. Ge, T. Nishinaga, C. Huo, Z. Xu, J. He, M. Masaki, M. Washiyama, X. Xie, R. Xi, *Microgravity Q.* 3 (2–4) (1993) 161–165.

- [4] T. Duffar, I. Paret-Harter, P. Dusserre, *J. Crystal Growth* 100 (1990) 171.
- [5] V.S. Zemskov, M.R. Raukhan, I.V. Barmin, A.S. Senchenkov, I.L. Shul'pinn, L.M. Sorokin, *Fiz. Khim. Obrab. Mater.* 17 (1983) 56.
- [6] D.J. Larson, M. Dudley, B. Raghothamachar, J.I.D. Alexander, F.M. Carlson, D. Gillies, M.P. Volz, T.M. Ritter, D. DiMarzio, NASA Microgravity Materials Science Conference, NASA/CP-1999-209092, Huntsville, AL, 1998, p. 409.
- [7] D. Gillies, S.L. Lehoczy, F.R. Szofran, D.J. Larson, C.-H. Su, Y.-G. Sha, H.A. Alexander, *SPIE* 2021 (1993) 10.
- [8] P. Dold, F.R. Szofran, K.W. Benz, *J. Crystal Growth* 234 (2001) 91.
- [9] T. Duffar, P. Dusserre, F. Picca, S. Lacroix, N. Giacometti, *J. Crystal Growth* 211 (2000) 434.
- [10] T. Duffar, P. Dusserre, N. Giacometti, *J. Crystal Growth* 223 (2001) 69.
- [11] F.R. Szofran, K.W. Benz, S.D. Cobb, A. Cröll, P. Dold, N. Kaiser, S. Motakef, M. Schweizer, M.P. Volz, L. Vujisic, J.W. Walker, NASA/CP-2001-210827. Proceedings of the NASA Microgravity Materials Science Conference, Huntsville, Alabama, USA, June 6–8, 2000, p. 573.
- [12] M.P. Volz, M. Schweizer, N. Kaiser, S.D. Cobb, L. Vujisic, S. Motakef, F.R. Szofran, *J. Crystal Growth*, accepted for publication.
- [13] N. Kaiser, A. Cröll, F.R. Szofran, S.D. Cobb, K.W. Benz, *J. Crystal Growth* 231 (2001) 448.
- [14] H. Wenzl, A. Fattah, D. Gustin, M. Mihelcic, W. Uelhoff, *J. Crystal Growth* 43 (1978) 607.
- [15] P. Barczy, *Material Sci. Forum* 329–330 (2000) 219.
- [16] E. Billig, *Proc. Soc. London A* 235 (1956) 37.
- [17] E. Scheil, *Z. Metallkunde* 34 (1942) 70.